Nanocrystal Growth

DOI: 10.1002/anie.201201025

An Electron Paramagnetic Resonance Spectroscopic Investigation on the Growth Mechanism of $NaYF_4$:Gd Nanocrystals**

Rajesh Komban, Johann P. Klare, Benjamin Voss, Jörg Nordmann, Heinz-Jürgen Steinhoff, and Markus Haase**

Understanding the growth mechanism of nanocrystals is a crucial factor for preparing nanoparticles with well-defined shapes, sizes and size distributions, and is therefore essential for their application in electronics, photonics, catalysis, as biological and chemical sensors.[1–3] In the classical model of crystal growth in solution, the particles increase in size by the reaction with monomers (i.e. ions, atoms or molecules) present in the solution. Different growth regimes are distinguished, depending on the concentration of the monomers and the reaction rates by which the monomers are added to or removed from the particle surface.[4–9] If the concentration of monomers is close to the equilibrium value for the mean particle size of the size distribution, Ostwald ripening is observed, that is, small particles dissolve and release monomers while the larger particles grow by the uptake of monomers. In the case of high supersaturation of monomer and diffusion-controlled reaction, narrow particle size distributions are obtained by a mechanism called "focusing" of the size distribution. High supersaturation can be achieved in the "hot-injection" synthesis of nanoparticles,[4–7,10] by the constant addition of new monomers during particle growth or by starting from a bimodal size distribution with a large difference between the two mean sizes.[10b,11]

Alternatively, smaller particles formed at early stages of the synthesis may join and fuse to larger particles. Examples for this growth mechanism are biomineralization processes as well as other particle-mediated crystallization pathways often involving an oriented attachment and/or a grain rotation process of the small particles.[12–15] In oriented attachment the small particles first align along a common crystallographic axis, presumably by spontaneous self-organization, before they join and coalesce.[13,16]

Recently, nearly monodisperse nanocrystals of sodium rare-earth metal fluorides ($NaREF_4$). are thoroughly investigated for biolabeling applications and for magnetic resonance imaging (MRI).[17–27] In the oleic acid-based synthesis of monodisperse $NaREF_4$ nanocrystals, very small $NaREF_4$ nanocrystals of either the cubic α-phase (e.g. $NaYF_4$) or the hexagonal β-phase (e.g. $NaGdF_4$) are formed as first product. The final hexagonal phase β-$NaREF_4$ nanocrystals grow from these intermediate particles at elevated temperatures.[28,29] For rod-shaped β-phase $NaREF_4$ nanocrystals prepared in a solvent mixture consisting of oleic acid, water, and alcohol,[30] it has been proposed that the particles form by the aggregation of small α-phase particles.[31] In the case of β-$NaREF_4$ nanocrystals prepared by the co-thermolysis of metal trifluoroacetate precursors in different oleic acid containing solvent mixtures, however, the growth of the β-$NaREF_4$ nanocrystals has been ascribed to the Ostwald ripening process, in which the monomers produced from the dissolution of the small α-$NaREF_4$ diffuse to the surface of the growing β-$NaREF_4$ nanocrystals.[28a,32,33]

In the present study we have investigated by electron paramagnetic resonance (EPR) spectroscopy the role of the small particles formed as intermediate material during the growth of the large β-phase particles. Since the paramagnetic Gd^{3+} ion exhibits a strong EPR response even at room temperature, we employed $NaGdF_4$ and Gd^{3+}-doped $NaYF_4$ nanocrystals as well as core–shell particles in our study. As the magnetic interaction between neighboring gadolinium ions leads to a strong broadening of the Gd EPR signal, we are able to detect whether the Gd^{3+} ions of a sample remain in close proximity during particle growth or not. We show that this dependence on the Gd–Gd distance can be used to distinguish between growth processes governed by the dissolution and re-crystallization of particles and those governed by the coalescence or oriented attachment of particles. EPR spectroscopy has already been used to investigate other paramagnetic ions in doped core and core–shell nanocrystals like manganese ions in MnO, CdSe, CdS/ZnS, ZnS/ZnS, ZnSe/CdSe nanoparticles.[34]

Throughout this study, purified small nanocrystals were used as single-source precursors for the preparation of the final β-phase particles. The synthesis procedures and the X-ray powder diffraction (XRD) data of all precursor and product particles are given in the Supporting Information (Data S1 and Figures S1 to S3).

The concentration of Gd^{3+} in the $NaYF_4$ lattice has a profound effect on the ESR signal of the nanoparticles. This is shown in Figure 1 where nanoparticles consisting of pure $NaGdF_4$ are compared with $NaYF_4$:Gd particles nominally doped with 10 and 1% Gd^{3+}, respectively. In general, the EPR spectrum of Gd^{3+} ($S = 7/2$) ions in a crystalline electric field is characterized by the Zeeman interaction with a *g*-

[*] Dr. R. Komban, B. Voss, J. Nordmann, Prof. Dr. M. Haase
Inorganic Chemistry 1, Institute of Chemistry
University of Osnabrueck
Barbarastrasse 7, 49076 Osnabrueck (Germany)
E-mail: markus.haase@uni-osnabrueck.de
Dr. J. P. Klare, Prof. Dr. H.-J. Steinhoff
Institute of Physics, University of Osnabrueck
Barbarastrasse 7, 49076 Osnabrueck (Germany)
E-mail: hsteinho@uni-osnabrueck.de

[**] We thank H. Eickmeier and M. Gather, University of Osnabrueck (Germany), for TEM investigations and X-ray powder diffraction analysis, respectively.

Supporting information for this article is available on the WWW under http://dx.doi.org/10.1002/anie.201201025.

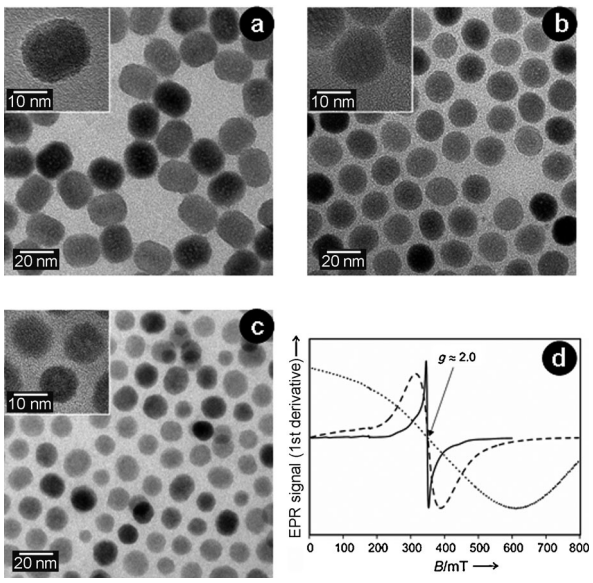

Figure 1. a–c) TEM images of a) $NaYF_4$:Gd(1%) particles, b) $NaYF_4$:Gd(10%) particles and c) $NaGdF_4$ particles. d) Normalized EPR spectra of $NaYF_4$:Gd(1%) particles (——), $NaYF_4$:Gd(10%) particles (- - - -) and $NaGdF_4$ particles (•••••). The width of the EPR spectra increases with the Gd^{3+} concentration because of the increased magnetic interaction of adjacent Gd^{3+} ions. All materials were prepared from small precursor particles having the same composition as the product.

value close to 2, and the zero-field splitting leading to the fine structure of the resonance spectrum. For weak crystal fields the corresponding X-band (9 GHz) EPR powder signal consists of a broad spectrum with a dominant resonance at g of about 2 as observed for the $NaYF_4$:Gd particles doped with 1% Gd^{3+} (Figure 1d).[35] The width of the EPR signal increases for nanocrystals doped with 10% Gd^{3+} and even stronger for pure $NaGdF_4$ particles because of the decrease of the average Gd–Gd distances and the corresponding increase of the magnetic interaction (i.e., dipolar interaction and isotropic exchange interactions) between the Gd^{3+} ions.[36] Moreover, Figure 1 shows that the particle size decreases slightly with increasing concentration of Gd^{3+}. Similar observations have been reported by Liu and co-workers who showed that the concentration of Gd^{3+} ions affects the growth of $Na(Y,Gd)F_4$ nanorods.[28b]

Qualitatively, a similar result is obtained with the much smaller precursor particles having a size of only 3–4 nm. The top part of Figure 2 shows TEM images and the EPR spectra of $NaYF_4$:Gd(1%) precursor particles and of a 1:99 mixture of $NaGdF_4$ and EPR-inactive $NaYF_4$ precursor particles. Again, the weakly doped $NaYF_4$:Gd(1%) particles show a dominating narrow Gd EPR signal in the $g = 2$ region (black line in Figure 2a) whereas the EPR signal of the $NaGdF_4$ particles in the mixture is very broad (Figure 2b). Due to its large width the EPR spectrum of the $NaGdF_4$ particles (additional gray line in Figure 2a) is much less intense than the spectrum of the $NaYF_4$:Gd(1%) particles and displays more noise when both spectra are normalized to the same intensity (compare black lines in Figure 2a and Figure 2b). Undiluted $NaGdF_4$ particles show a similar but, of course,

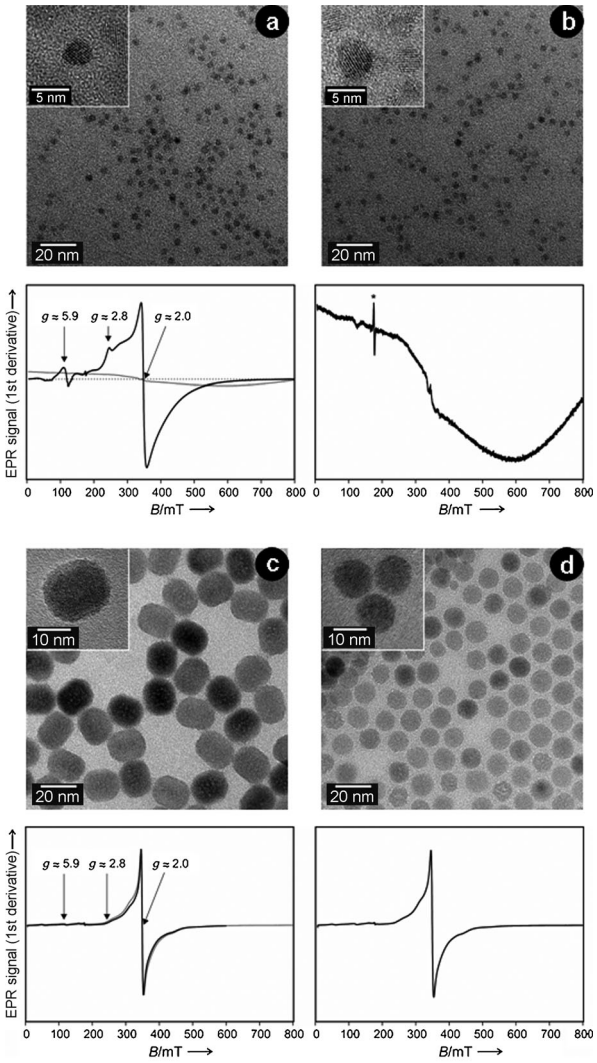

Figure 2. Top: TEM images and normalized EPR spectra (black lines) of a) $NaYF_4$:Gd(1%) precursor particles and of b) the 1:99 mixture of $NaGdF_4$ precursor particles and EPR-inactive $NaYF_4$ precursor particles. Bottom: TEM images and EPR spectra of the $NaYF_4$:Gd(1%) product particles obtained from (a) and (b), respectively. For a better comparison, the EPR spectra of part (b) and (d) are also given without normalization (i.e., drawn to scale) as additional gray lines in the spectra of part (a) and (c). The asterisk denotes an impurity signal of the microwave cavity present in all spectra at 175 mT.

much stronger and less noisy EPR spectrum (Figure S4 in the Supporting Information). Both spectra show contributions in the $g \geq 2.8$ region, which indicates the presence of Gd^{3+} ions in lattice sites different from bulk sites (see also Figure S5).[35] These contributions are more pronounced for the small precursor particles (Figure 2a) as will be discussed below.

We have now used the small particles shown in the upper part of Figure 2 as precursors for the preparation of large nanoparticles. Thus, in one case a 1:99 mixture of small $NaGdF_4$ and $NaYF_4$ particles and in the other case small particles of $NaYF_4$:Gd(1%) were heated for 20 min at 320 °C in an oleic acid/octadecene solvent mixture (see the Experimental Section for details). The products, which contain 1% Gd^{3+} in both cases, not only display narrow particle size

distributions (Figure 2c and d) but also EPR signals with nearly identical shape and intensity (black lines in Figure 2c and d). The latter is most evident when both spectra are superimposed (black line and gray line in Figure 2c). Obviously, the interaction of the Gd^{3+} ions and, hence, the distribution of Gd–Gd distances in both samples are similar, independent of the different starting materials. Interestingly, both EPR spectra display a narrow line width indicating that in both cases the magnetic interaction of the Gd^{3+} ions is weak. This clearly shows that the small $NaGdF_4$ particles are not incorporated into the large particles as intact building blocks, because in this case the Gd^{3+} in the subunits of $NaGdF_4$ would show the same strong magnetic interaction as before. Instead, the EPR signals reveal that in both cases the concentration of Gd^{3+} ions in the product particles is low and similar to the concentration in the small $NaYF_4$:Gd(1%) precursor particles. Obviously, the small $NaGdF_4$ and $NaYF_4$ particles dissolve before the large particles are formed. As the main result of this study, we can therefore provide direct proof that the large $NaREF_4$ particles are formed by a dissolution/recrystallization process as given in Scheme 1.

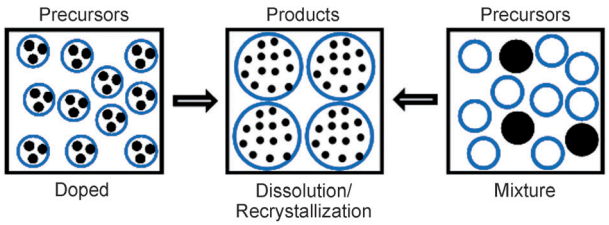

Scheme 1. The EPR results prove that the formation of the product particles follows a dissolution/recrystallization mechanism.

The EPR spectra of the $NaYF_4$:Gd(1%) samples also indicate, however, that the Gd^{3+} dopant ions are not homogeneously distributed inside the particles. The latter is deduced from the width of the EPR signals in Figure 2c and d displaying tails which decrease in intensity much less slowly than expected for isolated Gd^{3+} ions in lattice sites with high symmetry. In the present paper the details of the dopant distribution were not further investigated, since the almost identical shape and width of both EPR spectra indicate that the distribution is not much affected by the two different preparation methods (Figure 2c). Note, however, that a non-statistical dopant distribution has already been reported by van Veggel and co-workers for Ln^{3+} ions in $NaGdF_4$:Ln nanoparticles.[37]

We have already mentioned above that the small 3–4 nm particles of $NaYF_4$:Gd(1%) in Figure 2a display much stronger EPR resonances in the $g > 2.8$ region than the larger $NaYF_4$:Gd(1%) particles (bottom part of Figure 2). This indicates that particles with a very large surface-to-bulk ratio contain Gd^{3+} ions in sites with different symmetry and/or crystal fields.[35] In our case, lattice sites in the interior of the particles are expected to differ from those at the surface. To investigate how the particle surface affects the EPR spectrum, we prepared $NaYF_4$/$NaGdF_4$ core–shell particles with different shell thickness. In Figure 3 the TEM images and

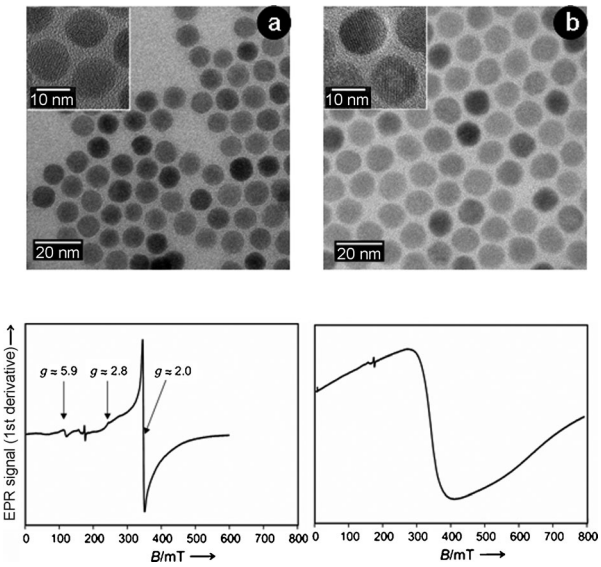

Figure 3. TEM images (top) and EPR spectra (bottom) of core–shell particles composed of an EPR-inactive $NaYF_4$ core and a Gd^{3+} containing surface layer. a) $NaYF_4$ particles after reaction ("shell growth") with a very small amount of $NaGdF_4$ precursor particles. b) $NaYF_4$ particles after reaction with a larger amount of $NaGdF_4$ precursor particles, resulting in a shell with nominal thickness of 1 nm.

EPR spectra of large $NaYF_4$ particles with a very thin "shell" (nominally 0.02 nm thick) are compared to those bearing a broader, approximately 1 nm thick shell. In both cases the shell was grown from small $NaGdF_4$ precursor particles which show a broad EPR signal as given in Figure 2b and Figure S4 in the Supporting Information. However, the resulting core–shell particles with thin "shell" display a narrow EPR signal (Figure 3a) which confirms our conclusion from above that the small $NaGdF_4$ precursor particles dissolve during the reaction. Moreover, the spectrum displays the same additional resonances at low field ($g > 2.8$) as the EPR spectrum of the small $NaYF_4$:Gd(1%) particles (Figure 2a), again indicating that this contribution is caused by Gd^{3+} ions at or very close to the particle surface. The spectrum in Figure 3a is in fact very similar to the EPR spectrum of the small $NaYF_4$:Gd(1%) particles (Figure 2a) indicating that a surface layer of weakly Gd^{3+}-doped $NaYF_4$ has formed. Since the concentration of dissolving $NaGdF_4$ precursor particles is small in this case, it is indeed likely that also Y^{3+} ions are released from the surface of the core particle during the reaction. When the shell thickness is increased to approximately 1 nm by employing a larger amount of $NaGdF_4$ precursor particles, the EPR signal of Gd^{3+} broadens again (Figure 3b). The enhanced magnetic interaction is in accord with a high Gd^{3+} concentration in the shell. We emphasize that the EPR spectrum of the core–shell particles in Figure 3b is not altered by an additional heating step (320°C, 20 min) after the synthesis (Figure S6 in the Supporting Information). This shows that diffusion of Gd^{3+} ions in the solid state, that is, from the $NaGdF_4$ shell into the $NaYF_4$ core, is negligible under our synthesis conditions.

In conclusion we have shown that the magnetic interaction of rare-earth metal ions, measured by EPR spectros-

copy, can be used to investigate the growth of nanocrystals. In the case of $Na(Y,Gd)F_4$ nanocrystals prepared in an oleic acid-based reaction medium, the final particles are formed by a dissolution/recrystallization process rather than the oriented attachment of small particles.

Received: February 7, 2012
Revised: April 20, 2012
Published online: May 22, 2012

Keywords: core–shell heterostructures · EPR spectroscopy · growth mechanism · nanoparticle · upconversion

[1] a) H. Goesmann, C. Feldmann, *Angew. Chem.* **2010**, *122*, 1402; *Angew. Chem. Int. Ed.* **2010**, *49*, 1362; b) D. V. Talapin, J. S. Lee, M. V. Kovalenko, E. V. Shevchenko, *Chem. Rev.* **2010**, *110*, 389; c) J. Lee, P. Hernandez, J. Lee, A. O. Govorov, N. A. Kotov, *Nat. Mater.* **2007**, *6*, 291; d) J. Park, J. Joo, S. G. Kwon, Y. Jang, T. Hyeon, *Angew. Chem.* **2007**, *119*, 4714; *Angew. Chem. Int. Ed.* **2007**, *46*, 4630; e) J. Luther, P. K. Jain, T. Ewers, A. P. Alivisatos, *Nat. Mater.* **2011**, *10*, 361; f) A. H. Fu, W. W. Gu, B. Boussert, K. Koski, D. Gerion, L. Manna, M. Le Gros, C. A. Larabell, A. P. Alivisatos, *Nano Lett.* **2007**, *7*, 179; g) J. S. Tans, R. M. Verschueren, C. Dekker, *Nature* **1998**, *393*, 49; h) B. Tian, T. J. Kempa, C. M. Lieber, *Chem. Soc. Rev.* **2009**, *38*, 16; i) H. Yan, H. S. Choe, S. W. Nam, Y. Hu, S. Das, J. F. Klemic, J. C. Ellenbogen, C. M. Lieber, *Nature* **2011**, *470*, 240; j) P. R. Brown, R. R. Lunt, T. P. Osedach, D. D. Wanger, L. Y. Chang, M. G. Bawendi, V. Bulovic, *Nano Lett.* **2011**, *11*, 2955.

[2] a) A special Issue on Nanoscale Materials: *Acc. Chem. Res.* **1999**, *32*, 387 – 454; b) *Nanoscale Materials in Chemistry*, 2nd ed. (Ed.: K. J. Klabunde), Wiley-Interscience, New York, **2009**; c) *Nanoparticles* (Ed.: G. Schmid), Wiley-VCH, Weinheim, **2004**.

[3] a) C. Sönnichsen, B. M. Reinhard, J. Liphardt, A. P. Alivisatos, *Nat. Biotechnol.* **2005**, *23*, 741; b) M. Bruchez, Jr., M. Moronne, P. Gin, S. Weiss, A. P. Alivisatos, *Science* **1998**, *281*, 2013; c) H. S. Choi, W. Liu, F. Liu, K. Nasr, P. Misra, M. G. Bawendi, J. V. Frangioni, *Nat. Nanotechnol.* **2010**, *5*, 42; d) Z. Popović, W. Liu, V. P. Chauhan, J. Lee, C. Wong, A. B. Greytak, N. Insin, D. G. Nocera, D. Fukumura, R. K. Jain, M. G. Bawendi, *Angew. Chem.* **2010**, *122*, 8831; *Angew. Chem. Int. Ed.* **2010**, *49*, 8649; e) B. Tian, T. Cohen-Karni, Q. Qing, X. Duan, P. Xie, C. M. Lieber, *Science* **2010**, *329*, 830.

[4] a) X. Peng, J. Wickham, A. P. Alivisatos, *J. Am. Chem. Soc.* **1998**, *120*, 5343; b) Z. A. Peng, X. Peng, *J. Am. Chem. Soc.* **2002**, *124*, 3343; c) Y. Xia, Y. Xiong, B. Lim, S. E. Skrabalak, *Angew. Chem.* **2009**, *121*, 62; *Angew. Chem. Int. Ed.* **2009**, *48*, 60.

[5] D. V. Talapin, A. L. Rogach, M. Haase, H. Weller, *J. Phys. Chem. B* **2001**, *105*, 12278.

[6] P. Dagtepe, V. Chikan, *J. Phys. Chem. C* **2010**, *114*, 16263.

[7] a) S. G. Kwon, T. Hyeon, *Acc. Chem. Res.* **2008**, *41*, 1696; b) S. G. Kwon, T. Hyeon, *Small* **2011**, *7*, 2685.

[8] I. M. Lifshitz, V. V. Slyozov, *J. Phys. Chem. Solids* **1961**, *19*, 35.

[9] C. Z. Wagner, *Elektrochem.* **1961**, *65*, 581.

[10] a) C. de Mello Donegá, P. Liljeroth, D. Vanmaekelbergh, *Small* **2005**, *1*, 1152; b) M. D. Clark, S. K. Kumar, J. S. Owen, E. M. Chan, *Nano Lett.* **2011**, *11*, 1976; c) P. Reiss, M. Protiére, L. Li, *Small* **2009**, *5*, 154.

[11] a) D. Tonti, M. B. Mohammed, A. Al-Salman, P. Pattison, M. Chergui, *Chem. Mater.* **2008**, *20*, 1331; b) H. L. Wang, D. Ning, S. L. Feng, *J. Cryst. Growth* **2000**, *209*, 630; c) H. G. Zhao, M. Chaker, D. L. Ma, *J. Phys. Chem. C* **2009**, *113*, 6497; d) C. Tuinenga, J. Jasinski, T. Iwamoto, V. Chikan, *ACS Nano* **2008**, *2*, 1411; e) J. Thessing, J. H. Qian, H. Y. Chen, N. Pradhan, X. G. Peng, *J. Am. Chem. Soc.* **2007**, *129*, 2736.

[12] a) T. Wang, H. Coelfen, M. Antonietti, *J. Am. Chem. Soc.* **2005**, *127*, 3246; b) H. Cölfen, M. Antonietti, *Angew. Chem.* **2005**, *117*, 5714; *Angew. Chem. Int. Ed.* **2005**, *44*, 5576; c) H. Cölfen, S. Mann, *Angew. Chem.* **2003**, *115*, 2452; *Angew. Chem. Int. Ed.* **2003**, *42*, 2350; d) A. W. Xu, M. Antonietti, H. Cölfen, Y. P. Fang, *Adv. Funct. Mater.* **2006**, *16*, 903.

[13] a) J. F. Banfield, S. A. Welch, H. Zhang, T. T. Ebert, R. L. Penn, *Science* **2000**, *289*, 751; b) R. L. Penn, J. F. Banfield, *Science* **1998**, *281*, 969; c) R. L. Penn, J. F. Banfield, *Geochim. Cosmochim. Acta* **1999**, *63*, 1549.

[14] H. Kuhn, G. Baero, H. Gleiter, *Acta Metall.* **1979**, *27*, 959.

[15] J. Fang, B. Ding, H. Gleiter, *Chem. Soc. Rev.* **2011**, *40,* 5347.

[16] a) M. A. Sliem, A. Chemseddine, U. Bloeck, R. A. Fischer, *CrystEngComm* **2011**, *13*, 483; b) C. Pacholski, A. Kornowski, H. Weller, *Angew. Chem.* **2002**, *114*, 1234; *Angew. Chem. Int. Ed.* **2002**, *41*, 1188; c) A. Narayanaswamy, H. Xu, N. Pradhan, X. Peng, *Angew. Chem.* **2006**, *118*, 5487; *Angew. Chem. Int. Ed.* **2006**, *45*, 5361; d) K. S. Cho, D. V. Talapin, W. Gaschler, C. B. Murray, *J. Am. Chem. Soc.* **2005**, *127*, 7140; e) S. J. Liu, J. Y. Gorig, B. Hu, S. H. Yu, *Cryst. Growth Des.* **2009**, *9*, 203; f) X. L. Hu, J. M. Gong, L. Z. Zhang, J. C. Yu, *Adv. Mater.* **2008**, *20*, 4845; g) X. D. Liang, L. Gao, S. W. Yang, J. Sun, *Adv. Mater.* **2009**, *21*, 2068.

[17] H. S. Mader, P. Kele, S. M. Saleh, O. S. Wolfbeis, *Curr. Opin. Chem. Biol.* **2010**, *14*, 582.

[18] A. Hischemöller, J. Nordmann, P. Ptacek, K. Mummenhoff, M. Haase, *J. Biomed. Nanotechnol.* **2009**, *5*, 278.

[19] M. Wang, C. C. Mi, W. X. Wang, C. H. Liu, Y. F. Wu, Z. R. Xu, C. B. Mao, S. K. Xu, *ACS Nano* **2009**, *3*, 1580.

[20] Z. Li, Y. Zhang, S. Jiang, *Adv. Mater.* **2008**, *20*, 4765.

[21] a) H. S. Qian, H. C. Guo, P. C.-L. Ho, R. Mahendran, Y. Zhang, *Small* **2009**, *5*, 2285; b) H. Hu, L. Xiong, J. Zhou, F. Li, T. Cao, C. Huang, *Chem. Eur. J.* **2009**, *15*, 3577.

[22] a) E. N. M. Cheung, R. D. A. Alvares, W. Oakden, R. Chaudhary, M. L. Hill, J. Pichaandi, G. C. H. Mo, C. Yip, P. M. Macdonald, G. J. Stanisz, F. C. J. M. van Veggel, R. S. Prosser, *Chem. Mater.* **2010**, *22*, 4728; b) N. J. J. Johnson, W. Oakden, G. J. Stanisz, R. S. Prosser, F. C. J. M. van Veggel, *Chem. Mater.* **2011**, *23*, 3714.

[23] Q. Zhan, J. Qian, H. Liang, G. Somesfalean, D. Wang, S. He, Z. Zhang, S. Andersson-Engels, *ACS Nano* **2011**, *5*, 3744.

[24] Z. Li, Y. Zhang, B. Shuter, N. M. Idris, *Langmuir* **2009**, *25*, 12015.

[25] Y. I. Park, J. H. Kim, K. T. Lee, K.-S. Jeon, H. B. Na, J. H. Yu, H. M. Kim, N. Lee, S. . Choi, S.-I. Baik, H. Kim, S. P. Park, B.-J. Park, Y. W. Kim, S. H. Lee, S.-Y. Yoon, I. C. Song, W. K. Moon, Y. D. Suh, T. Hyeon, *Adv. Mater.* **2009**, *21*, 4467.

[26] Q. Liu, Y. Sun, C. Li, J. Zhou, C. Li, T. Yang, X. Zhang, T. Yi, D. Wu, F. Li, *ACS Nano* **2011**, *5*, 3146.

[27] R. Kumar, M. Nyk, T. Y. Ohulchanskyy, C. A. Flask, P. N. Prasad, *Adv. Funct. Mater.* **2009**, *19*, 853.

[28] a) H. X. Mai, Y. W. Zhang, L. D. Sun, C. H. Yan, *J. Phys. Chem. C* **2007**, *111*, 13730; b) F. Wang, Y. Han, C. S. Lim, Y. Lu, J. Wang, J. Xu, H. Chen, C. Zhang, M. Hong, X. Liu, *Nature* **2010**, *463*, 1061; c) H. X. Mai, Y. W. Zhang, R. Si, Z. G. Yan, L. D. Sun, L. P. You, C. H. Yan, *J. Am. Chem. Soc.* **2006**, *128*, 6426; d) M. Haase, H. Schäfer, *Angew. Chem.* **2011**, *123*, 5928; *Angew. Chem. Int. Ed.* **2011**, *50*, 5808.

[29] S. Zeng, G. Ren, C. Xu, Q. Yang, *CrystEngComm* **2011**, *13*, 1384.

[30] a) L. Y. Wang, Y. D. Li, *Nano Lett.* **2006**, *6*, 1645; b) L. Y. Wang, Y. D. Li, *Chem. Mater.* **2007**, *19*, 727.

[31] X. Liang, X. Wang, J. Zhuang, Q. Peng, Y. D. Li, *Adv. Funct. Mater.* **2007**, *17*, 2757.

[32] a) G. S. Yi, G. M. Chow, *Adv. Funct. Mater.* **2006**, *16*, 2324; b) J. Shan, X. Qin, N. Yao, Y. Ju, *Nanotechnology* **2007**, *18*, 445607.

[33] J. Shan, Y. Ju, *Nanotechnology* **2009**, *20*, 275603.

[34] a) F. V. Mikulec, M. Kuno, M. Bennati, D. A. Hall, R. G. Griffin, M. G. Bawendi, *J. Am. Chem. Soc.* **2000**, *122*, 2532; b) Y. Yang, O. Chen, A. Angerhofer, Y. C. Cao, *J. Am. Chem. Soc.* **2006**, *128*, 12428; c) Y. Yang, O. Chen, A. Angerhofer, Y. C. Cao, *J. Am. Chem. Soc.* **2008**, *130*, 15649; d) A. López-Ortega et al., *J. Am. Chem. Soc.* **2010**, *132*, 9398; e) Z. Quan, Z. Wang, P. Yang, J. Lin, J. Fang, *Inorg. Chem.* **2007**, *46*, 1354; f) V. A. Vlaskin, R. Beaulac, D. R. Gamelin, *Nano Lett.* **2009**, *9*, 4376.
[35] C. M. Brodbeck, L. E. Iton, *J. Chem. Phys.* **1985**, *83*, 4285.
[36] a) H. Gustafsson, M. Ahrén, F. Söderlind, J. M. C. Gallego, P.-O. Käll, P. Nordblad, P.-O. Westlund, K. Uvdal, M. Engström, *J. Phys. Chem. C* **2011**, *115*, 5469; b) C. Filip, C. Kessler, F. Balibanu, P. Kleeman, A. Darabont, L. V. Giurgiu, M. Mehring, *Physica B* **1996**, *222*, 16 – 30; c) G. Ren, S. Zeng, J. Hua, *J. Phys. Chem. C* **2011**, *115*, 20141.
[37] a) C. Dong, J. Pichaandi, T. Regier, F. C. J. M. van Veggel, *J. Phys. Chem. C* **2011**, *115*, 15950; b) K. A. Abel, J.-C. Boyer, F. C. J. M. van Veggel, *J. Am. Chem. Soc.* **2009**, *131*, 14644; c) K. A. Abel, J.-C. Boyer, C. M. Andrei, F. C. J. M. van Veggel, *J. Phys. Chem. Lett.* **2011**, *2*, 185.

